University College London

Computational Modelling for Biomedical Imaging - Individual Report

---

Author:
Răzvan Valentin Marinescu
razvan.marinescu.14@ucl.ac.uk

EPSRC Centre for Doctoral Training in Medical Imaging
University College London

April 23, 2015

Introduction

Radiation therapy uses ionizing radiation to control or kill cancerous cells. It works by dmaging the DNA of the cancerous tissue leading to cellular death. In order to spare normal tissue, radiation beams are aimed from various angles and intersect at the tumour, providing a much larger dose than in the surrounding tissue. However, it is sometimes not straightforward to localise the turmour, especially due to respiratory motion. Over time, several solutions have been proposed to deal with the problem or lung motion. The simplest approach is for the patient to hold her/his breath, but this limits the acquisition time to less than 30 seconds. Implanted markers could also be used to track the tumour [1], but this is an invasive procedure that carries a certain ammount of risk. An alternative solution is to use correspondence models, which try to predict the motion of the lung based on input from a surrogate signal, which is easy to acquire during the RT intervention. The correspondence model is first trained using CT scans and the surrogate signal, and then during the RT intervention it can predict the lung position using only the surrogate signal. A lot of research has previously been done in respiratory motion modelling using different correspondence models (linear [2], polynomial [3], B-spline [4]), imaging modalities (MR [5], CT [3]) or types of surrogate signals(single signal [2], respiratory phase [6]). The aim of the project is to evaluate how well polynomial and b-spline correspondence models can model the lung deformation.

Methods

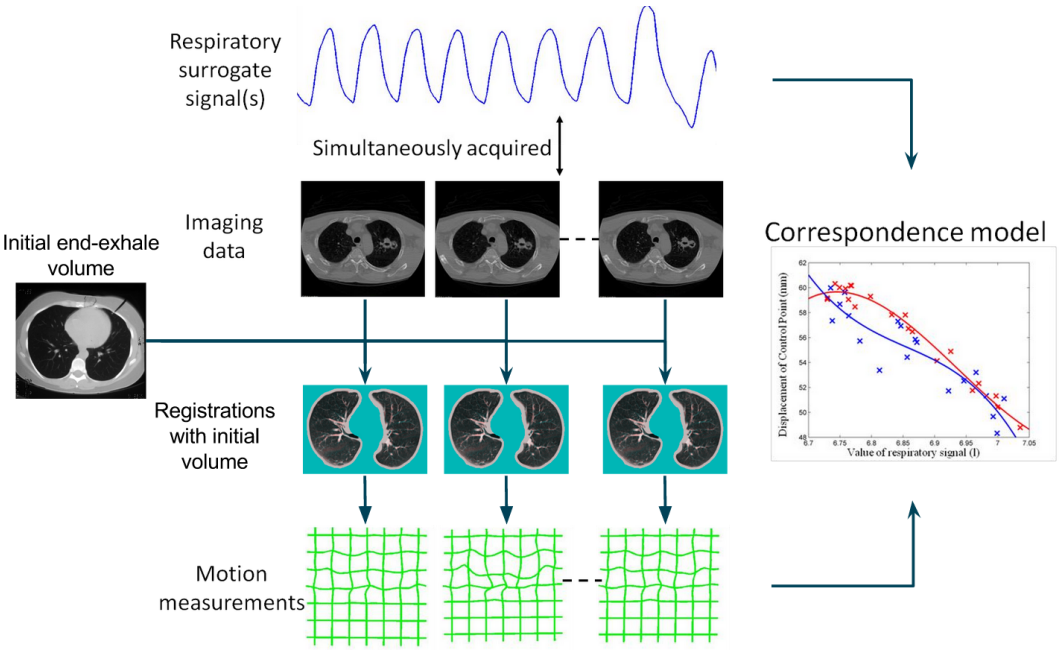

Figure 1: Diagram describing the motion model system. The respiratory surrogate signal and the Cine CT scans are acquired simoulatenously, and then these are registered with the initial end-exhale volume. The deformation grids that result from the registration and the surrogate signals are then used to build the correspondence motion model.

The imaging data given to us contained 40 Cine CT volumes acquired over 20 seconds at 5 different couch positions. Moreover, the initial end-exhale volume as well as registrations between this initial volume and the Cine CT volumes were provided. The surrogate signal was computed using the Vision RT system, and measures the volume between the chest surface and the couch. We were also given the gradient and the respiratory phase. We used this data to evaluate 9 different algorithms:

1. linear
2. quadratic
3. cubic
4. linear - phase separation
5. quadratic - phase separation
6. cubic - phase separation
7. B-spline
8. 2D linear
9. 2D quadratic

I fit the models for one voxel by solving the following GLM: $D = SC$ where D is the displacement along one direction, S is the matrix of surrogate signals and C are the coefficients. I chose to solve the GLM using the pseudo-inverse of $S^\top S$, giving $C = pinv(S^\top S)S^\top D$. I used the MATLAB function `pinv` because it can better handle singularities than the function `inv`. These 9 models have been fit for all CP displacements using a fast (vectorised) method where all the CP displacements are flattened into a huge matrix.

Results

Task 1 - Registration assessment

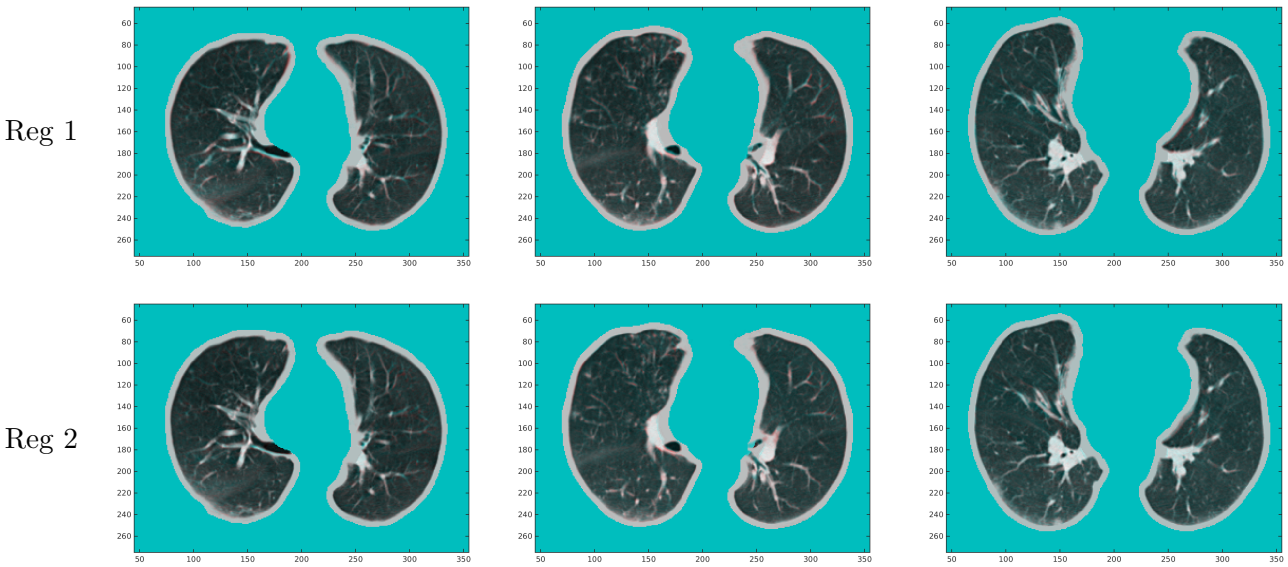

(a) Couch 1, volume 1, slice 66 (b) Couch 2, volume 5, slice 60 (c) Couch 3, volume 2, slice 49

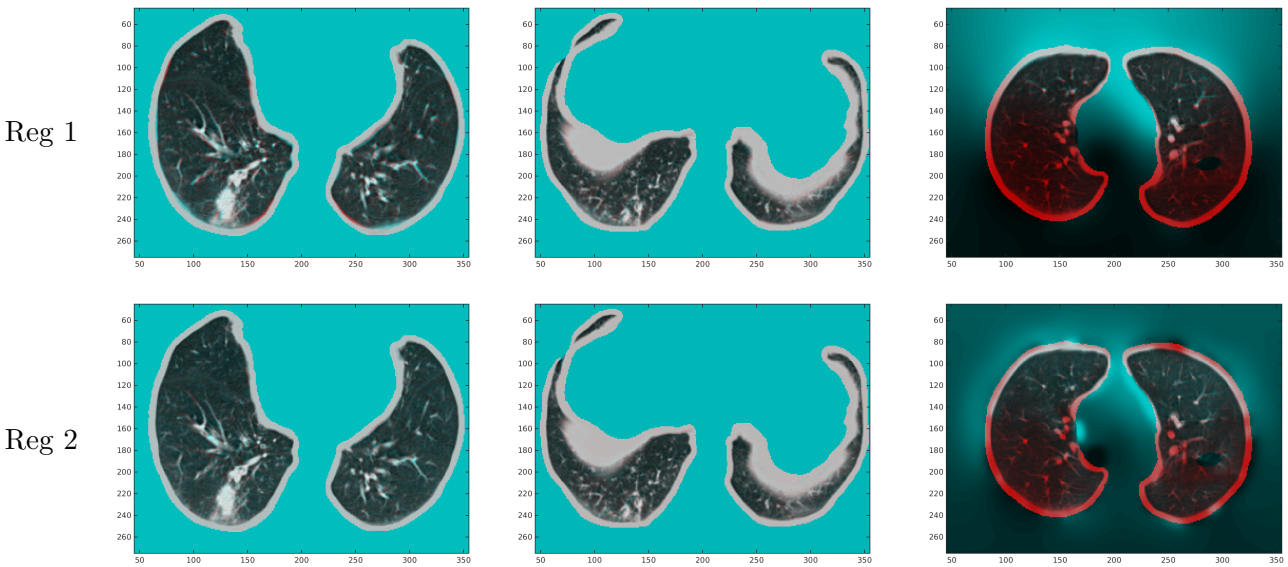

(d) Couch 4, volume 8, slice 37 (e) Couch 5, volume 4, slice 25 (f) Couch 1, volume 6, slice 76

Figure 2: Registration results at several different slices and volumes for each couch position. For each subfigure, registration 1 and 2 are shown in the upper and lower figures respectively. Registration worked fine in these examples apart from the slice in subfigure 2f.

Figure 2 shows the registration results for a few representative slices and volumes over all couch positions. Both registrations perform equally well in subfigures (2a - 2e), but yielded a bad registration for couch

1, volume 6, slice 76 in subfigure 2f. Similar bad registrations have been observed in the last slice of each volume, suggesting that the registration does not always work. The images show us that there is a considerable ammount of respiratory motion across different couch position and slices which needs to be modelled. The shape of the lung is also dramatically different across different couch positions, reaching a concave shape at couch 5. Nevertheless, the segmentation and registration worked fine even for these nonstandard slices.

Task 2 & 3 - Fitting the models

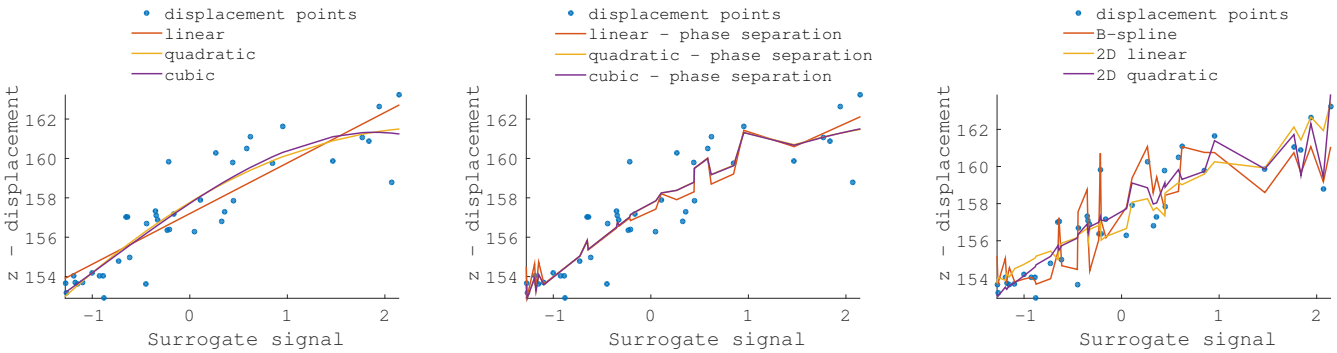

(a) Fit for couch position 1, voxel (30,40,33,1,3)

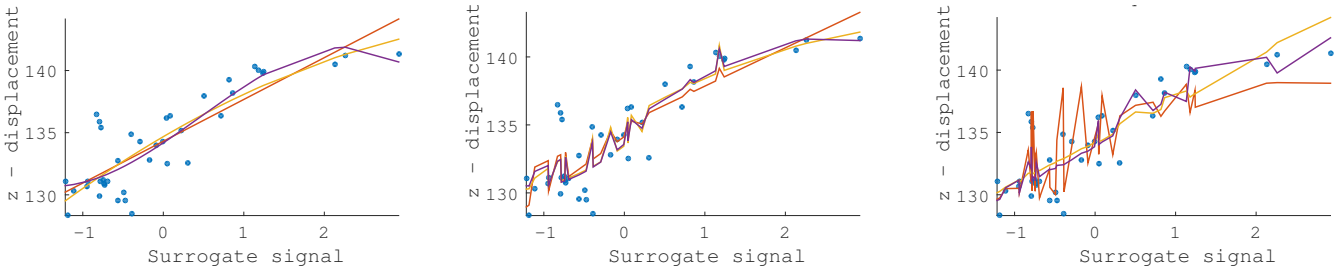

(b) Fit for couch position 2, voxel (30,40,28,1,3)

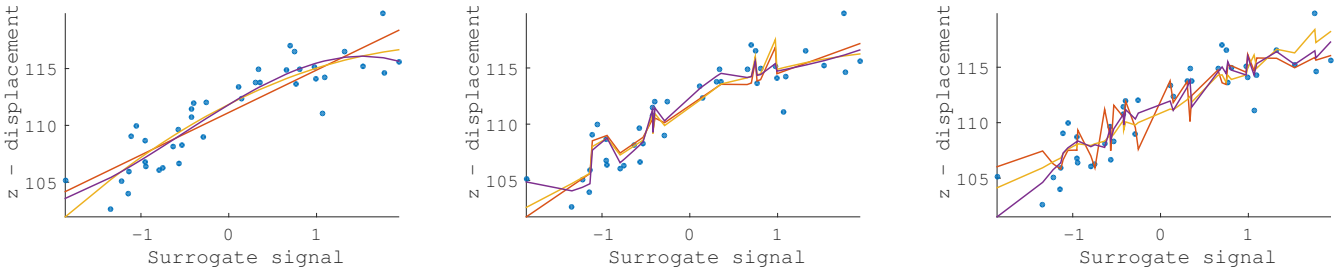

(c) Fit for couch position 3, voxel (30,40,23,1,3)

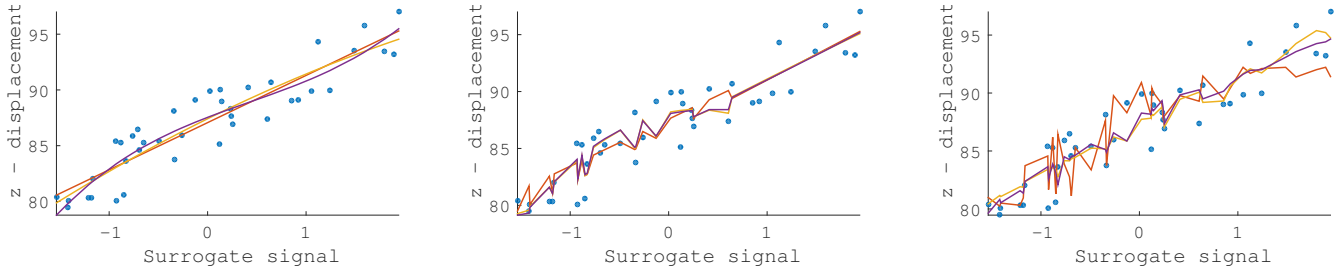

(d) Fit for couch position 4, voxel (30,45,18,1,3)

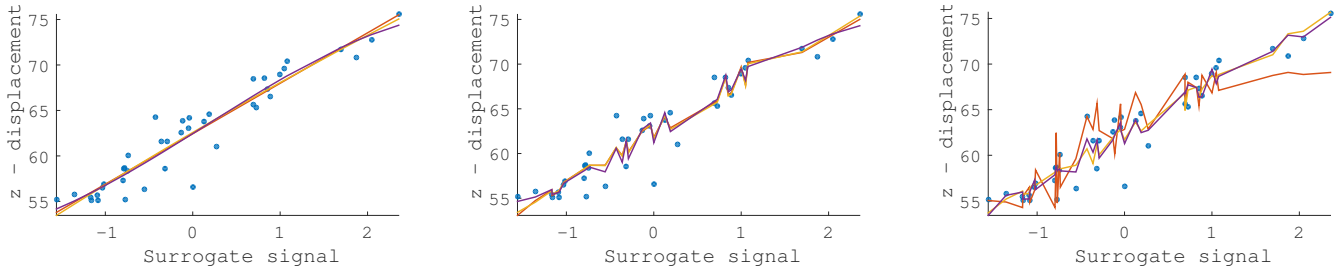

(e) Fit for couch position 5, voxel (30,45,13,1,3)

Figure 3: Fit of 9 different models across 5 voxels each from a different couch position. The first column shows the fit for the three basic models: linear, quadratic and cubic. The second column shows the same models with phase separation, while the last column shows the fit for the B-spline, 2D linear and 2D quadratic models.

Figure 3 shows the fit for the 9 different models.

The fit is plotted in figure 3 only for the given voxels for all the couch positions (one voxel/row with three groups of models for each plot).

The linear, quadratic and cubic models (plots in the column) give a reasonably good fit, especially for couch positions 4 and 5. The quadratic and cubic models don't differ much from the linear model, especially for voxels in couche positions 4 and 5. The phase separation models seem to fit outlier points better, but at the expense of extra parameters in the model. The B-spline and the 2D linear and quadratic models seem to fit the data best, but they run the risk of overfitting. The B-spline model seems to have a very oscilatory behaviour in the first few volumes, most evident in couch 2. In conclusion, all models fit these particular voxels well, and as we expected the more complex models give a better fit than the simpler models.

Task 4 - Evaluation of the motion models

Visual Assessment

Figure 4 shows the visual assessment for all the 9 models for couch 1, volume 1, slice 66. There is considerably more motion compared to the registration assessment in task 1. The results are quite good, with essentially no differences between the estimated defirmation across the models. The motion of the outer shape of the lung has been almost perfectly estimated, with tiny errors at the top corner of the right lung. More deformation errors are found at the vasculature of the right lung. We therefore conclude that all 9 models perform equally well.

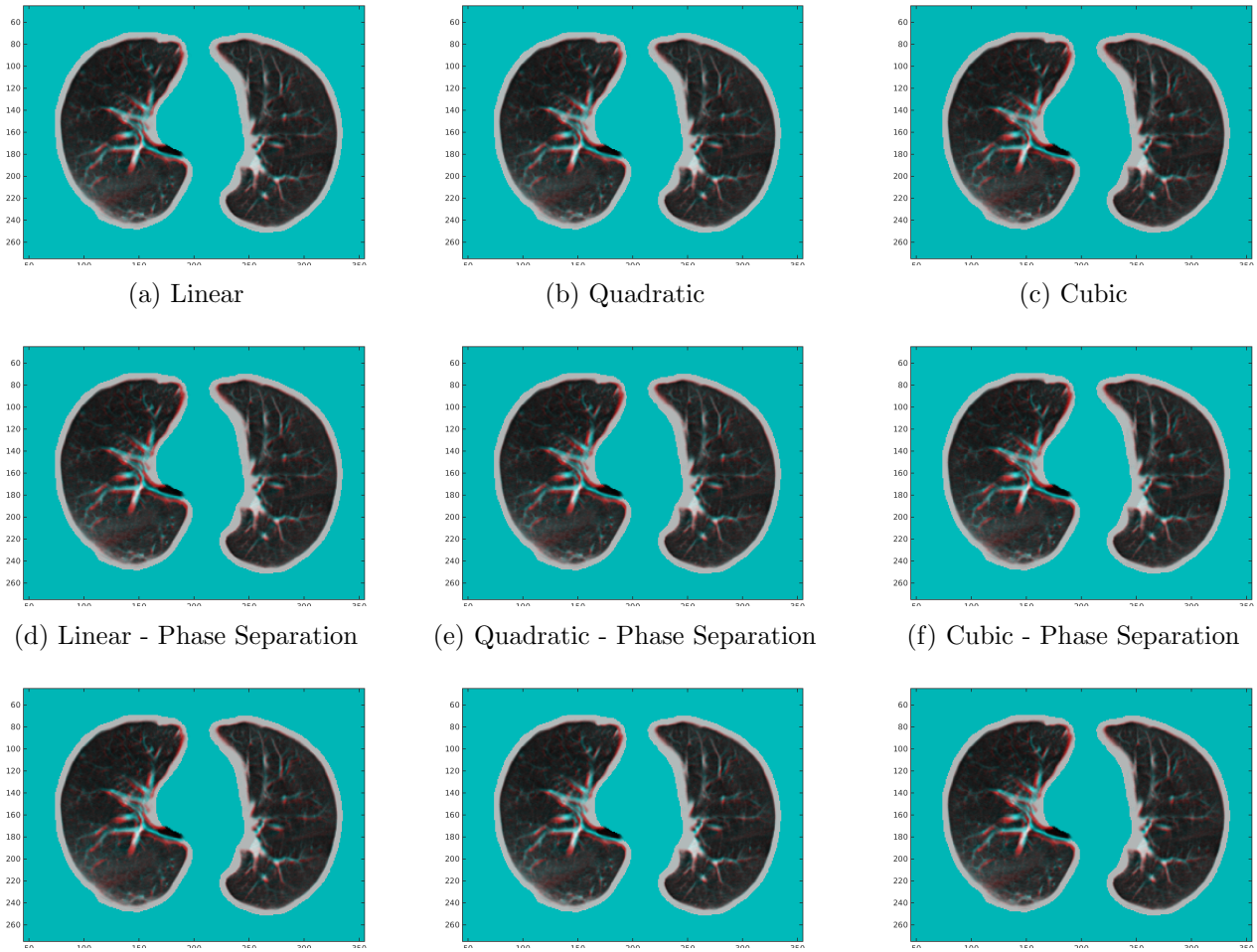

(a) Linear (b) Quadratic (c) Cubic

(d) Linear - Phase Separation (e) Quadratic - Phase Separation (f) Cubic - Phase Separation

(g) B-spline (h) Linear 2D (i) Quadratic 2D

Figure 4: Visual assessment of the 9 deformation models using leave-one out cross-validation on couch 1, volume 1, slice 66.

Deformation Field Error

Figure 5 shows the deformation field error for the 10 Cine CT volumes across all 5 couch positions. The left column shows the mean error, while the right column shows the standard deviation. The ammount of motion varies slightly across the Cine CT scans but is usually less than 3mm. Similarly, standard deviation is usually below 1.2. The B-spline model seems to have larger error means and standard deviations especially in volumes from couch positions 4 and 5. The other models have similar errors across all couch positions.

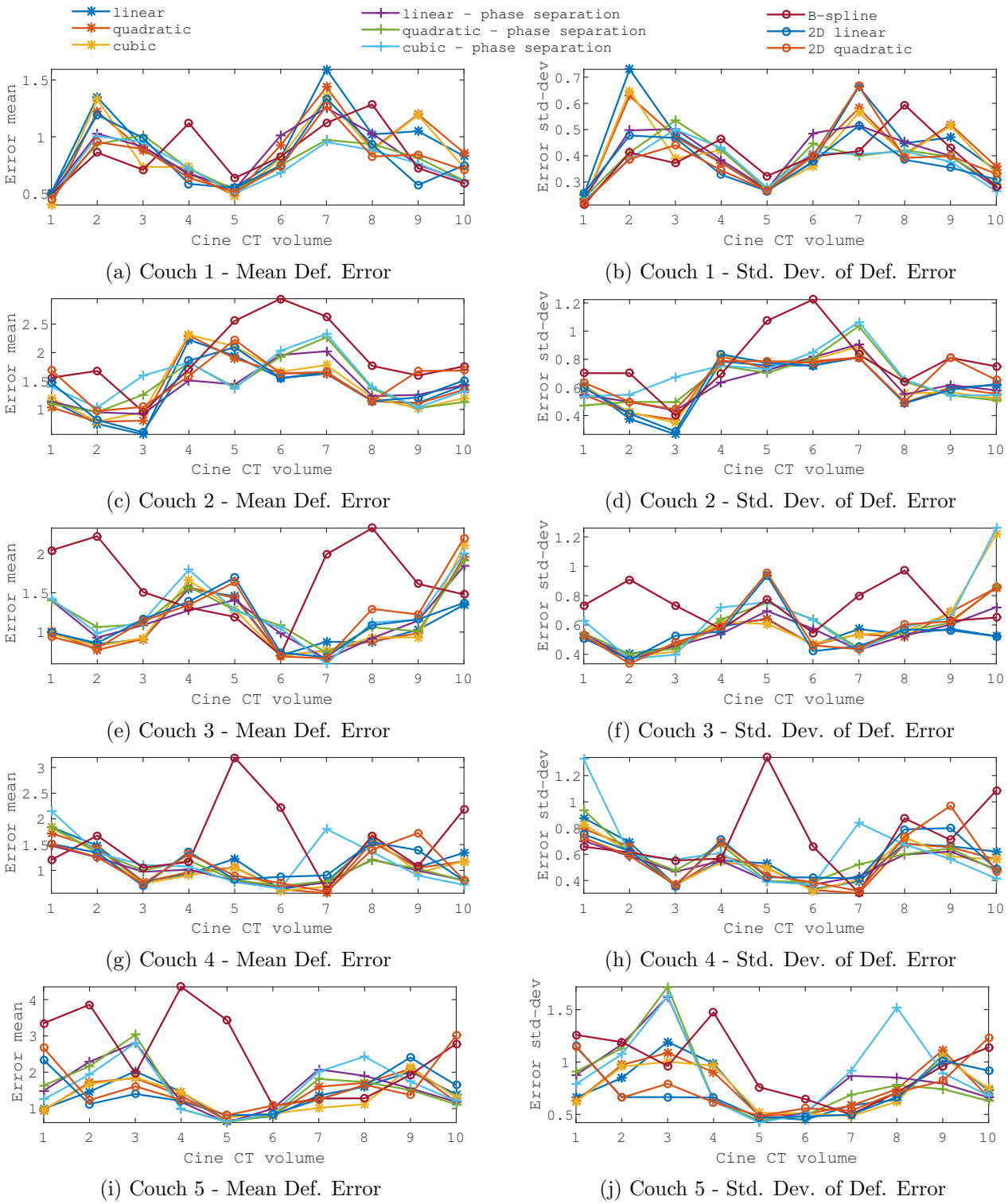

(a) Couch 1 - Mean Def. Error

(b) Couch 1 - Std. Dev. of Def. Error

(c) Couch 2 - Mean Def. Error

(d) Couch 2 - Std. Dev. of Def. Error

(e) Couch 3 - Mean Def. Error

(f) Couch 3 - Std. Dev. of Def. Error

(g) Couch 4 - Mean Def. Error

(h) Couch 4 - Std. Dev. of Def. Error

(i) Couch 5 - Mean Def. Error

(j) Couch 5 - Std. Dev. of Def. Error

Figure 5: Deformation Error mean and standard deviation for all 5 couch positions, 10 Cine CT volumes and 9 models.

Landmark Error

Figure 6 shows the landmark errors for all the 9 models across the 5 couch positions, this time using all 40 Cine CT volumes. Moreover, the landmark error using the original registration is also plotted in black. The landmark error is usually between 1 and 4mm. All models perform equally good, with no clear winner from the plots. In particular, the cubic - phase separation model seems to have a spike in landmark error at couch position 2, volume 24, which might be due to overfitting.

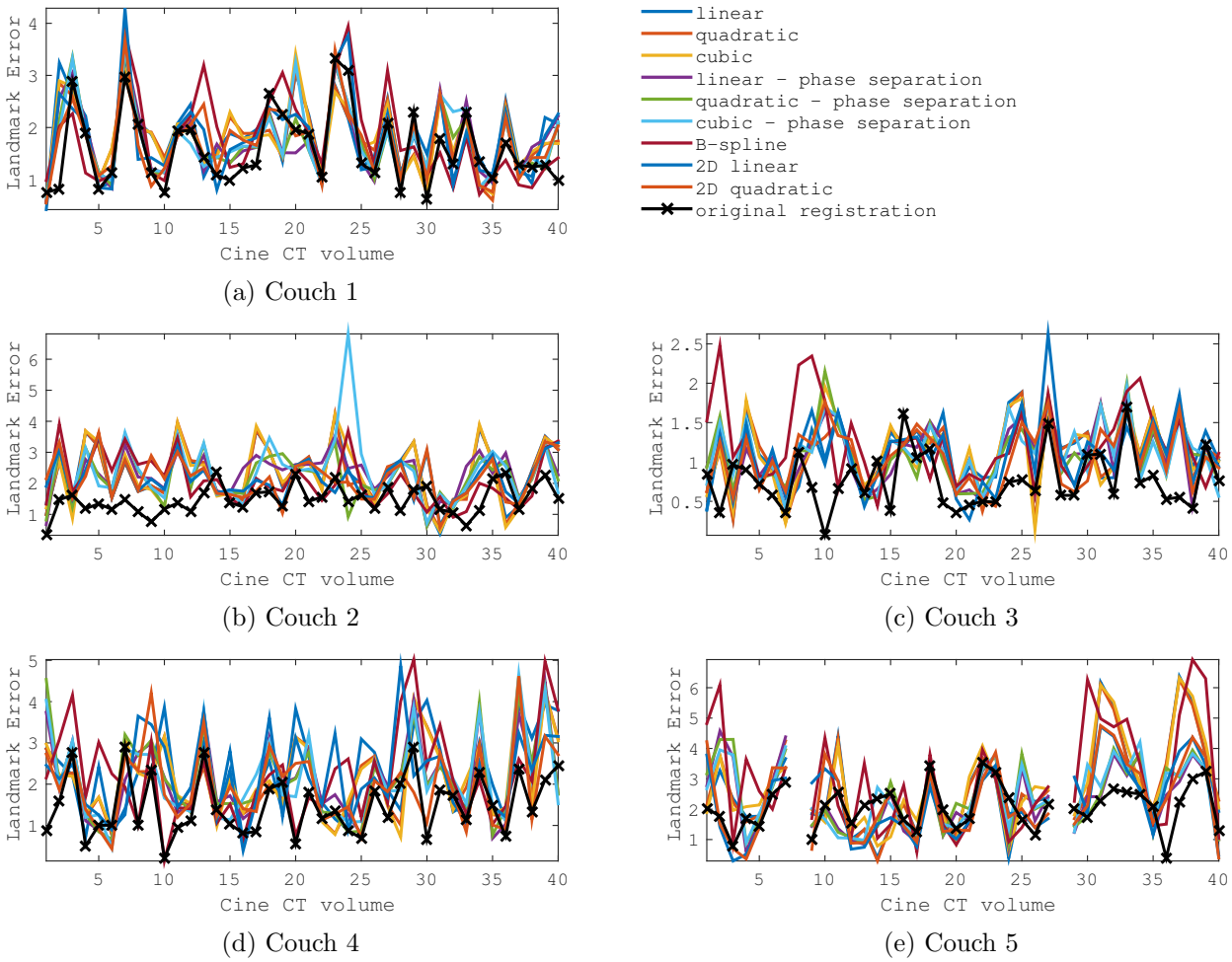

(a) Couch 1

(b) Couch 2

(c) Couch 3

(d) Couch 4

(e) Couch 5

Figure 6: Landmark error for all 5 couch positions, 40 Cine CT volumes and 9 models.

Model Ranking

Task 5 - Parameter uncertainty

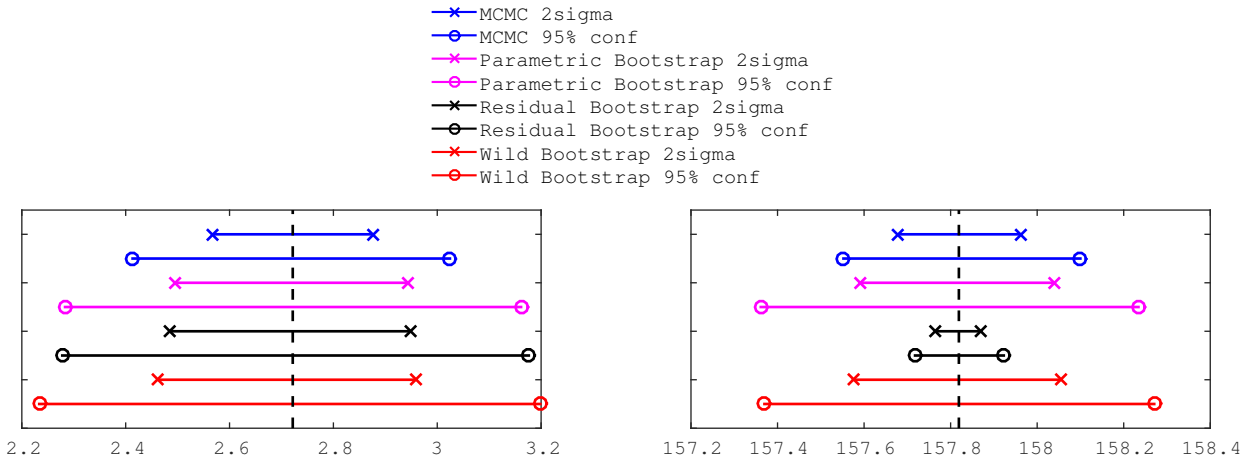

(a) Parameter 1 (b) Parameter 2

Figure 7: Parameter uncertainty for the linear model.

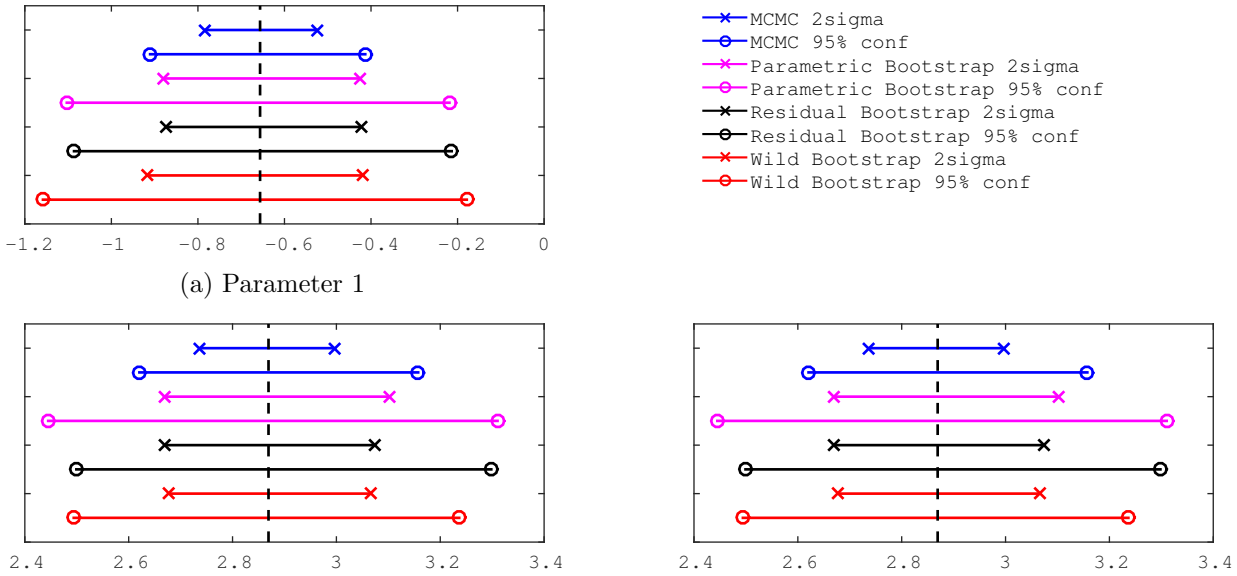

(a) Parameter 1

(b) Parameter 2 (c) Parameter 3

Figure 8: Parameter uncertainty for the quadratic model.

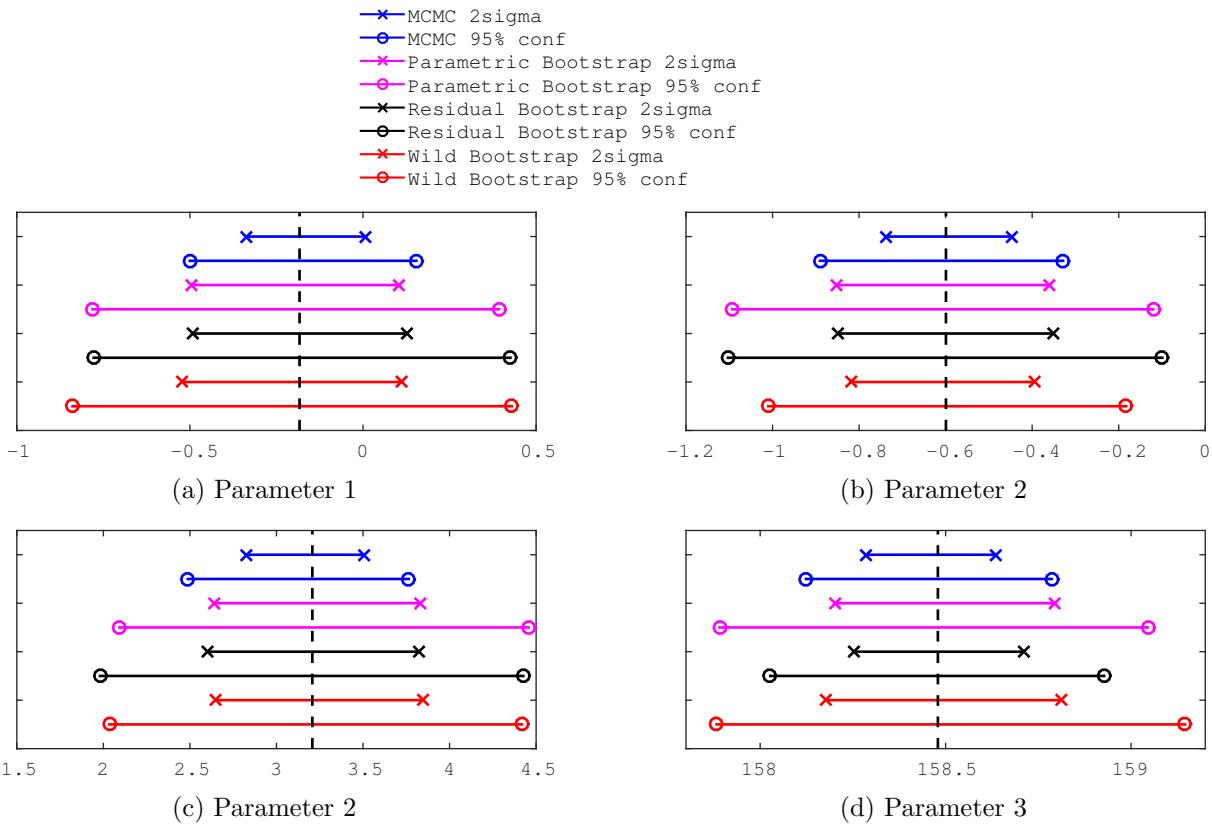

(a) Parameter 1

(b) Parameter 2

(c) Parameter 2

(d) Parameter 3

Figure 9: Parameter uncertainty for the cubic model.

Advanced tasks

Discussion

Bibliography

[1] Hiroki Shirato, Shinichi Shimizu, Tatsuya Kunieda, Kei Kitamura, Marcel van Herk, Kenji Kagei, Takeshi Nishioka, Seiko Hashimoto, Katsuhisa Fujita, Hidefumi Aoyama, et al. Physical aspects of a real-time tumor-tracking system for gated radiotherapy. *International Journal of Radiation Oncology* Biology* Physics*, 48(4):1187–1195, 2000.

[2] Achim Schweikard, Greg Glosser, Mohan Bodduluri, Martin J Murphy, and John R Adler. Robotic motion compensation for respiratory movement during radiosurgery. *Computer Aided Surgery*, 5(4):263–277, 2000.

[3] JR McClelland, AG Chandler, JM Blackall, S Ahmad, DB Landau, and DJ Hawkes. 4d motion models over the respiratory cycle for use in lung cancer radiotherapy planning. In *Medical Imaging*, pages 173–183. International Society for Optics and Photonics, 2005.

[4] Christian Buerger, RE Clough, Andrew P King, Tobias Schaeffter, and Claudia Prieto. Nonrigid motion modeling of the liver from 3-d undersampled self-gated golden-radial phase encoded mri. *Medical Imaging, IEEE Transactions on*, 31(3):805–815, 2012.

[5] Dirk Manke, Kay Nehrke, and Peter Börnert. Novel prospective respiratory motion correction approach for free-breathing coronary mr angiography using a patient-adapted affine motion model. *Magnetic Resonance in Medicine*, 50(1):122–131, 2003.

[6] Guy Shechter, Cengizhan Ozturk, Jon R Resar, and Elliot R McVeigh. Respiratory motion of the heart from free breathing coronary angiograms. *Medical Imaging, IEEE Transactions on*, 23(8):1046–1056, 2004.